

# Evaluation of tensile strength of fibreglass composites-hybrid due to differences in sand size



Yusrizal Muchlis<sup>ab</sup> | Husaini<sup>ac</sup> | Nurdin Ali<sup>ac</sup> | Akhyar<sup>ac</sup>  

<sup>a</sup>Doctoral Program, School of Engineering, Universitas Syiah Kuala, Jl. Syech Abdurrauf No. 7, Darussalam, Banda Aceh, 23111, Indonesia.

<sup>b</sup>Department of Mechanical Engineering, Universitas Abulyatama, Banda Aceh, Indonesia.

<sup>c</sup>Department of Mechanical Engineering, Universitas Syiah Kuala, Jl. Syech Abdurrauf no.7 Darussalam, Banda Aceh 23111, Indonesia.

**Abstract** Hybrid composites are a combination of two or more types of fibers to create alternative materials. Therefore, this study aimed to investigate the potential of hybrid fiber-particle composites to acquire new tensile properties derived from both types of fibers and particles. In this study, CSM300 glass fiber reinforcement was combined with sand, incorporating varying particle sizes to create a hybrid fiber reinforcement system. The analysis was carried out using five variations of sand particle sizes at 12, 16, 20, 24, and 40 (mesh size). The layers were arranged as RS+FG-SP-FG+RS (resin + fiberglass - sand particle #12, #16, #20, #24, #40 - resin + fiberglass), each incorporated in polyester resin using the manual press molding method at room temperature. The results showed that the highest tensile strength of the hybrid system (RS+FG-SP#16-FG+RS: 49.49 MPa) was achieved by combining both types of glass fiber and sand with #16 (sand mesh size). Furthermore, the maximum yield stress of 44.84 MPa and percent elongation of 10.17% were obtained at #16 and #12 sand mesh size, respectively. Research limitations/implications: The tensile strain-to-failure showed a significant increase from 0.22% at the beginning of the mesh particle size variation and reached a maximum for the fiberglass hybrid composite at #16 sand mesh particle size. For practical implications, the utilization of this technology requires the critical adjustment of sand diameter for industrial hybrid composite applications to achieve desired product specifications. Generally, the tensile index showed an increase at the initial sand size, reaching its peak at 0.35 mm (#16), followed by a decrease as the sand diameter is refined, with increasing mesh size.

**Keywords:** tensile strength, yield stress, percent elongation, fiberglass composites-hybrid, sand particle size

## 1. Introduction

Hybrid composites are a combination of several layers arranged in a specific number and unidirectional sequence. However, these composites have not been fully optimized, presenting the opportunity for further research and wider structural application of composite structures. A previous study has investigated the mechanical properties of two types of natural fibers, namely banana and kenaf. The specimens used were made with a size of 300 mm x 300 mm x 4 mm at a random and structured (plain weave) orientation. The experiment was conducted using six fiber variations, which included BP (Banana Plain), KP (Kenaf Plain), HP (Hybrid Plain), BR (Banana Random), KR (Kenaf Random), and HR (Hybrid Random). Based on the tensile strength test, the lowest results were obtained for BR and KR, ranging from 58 to 64 MPa, while the random hybrid composites reached a value of 68 MPa. In contrast, the plain weave variation showed a better value compared to the random counterpart, with BP, KP, and HP at, 74 MPa, 115 MPa, and 140 MPa, respectively. This indicated that the combination of two natural fibers in the form of a structured woven orientation demonstrated excellent good tensile strength (Alavudeenn et al., 2015).

Hybrid composites have also been developed using the hand lay-up manufacturing method to reduce synthetic materials that are not environmentally friendly while maintaining good structural strength. These composites were made with varying weight fractions of aramid (Kevlar)/kenaf, including ratios of 78/22 (H1), 60/40 (H2), 50/50 (H3), 26/74 (H4), 32/68 (H5), 100/0 and 0/100. The results of the tensile test showed that 100/0 (100% Kevlar) had the highest value of 240 MPa, while H1, H2, and H3 had values of 200 MPa, 150 MPa, and 100 MPa. Hybrid composite with a 50:50 ratio had lower values, including H4 at 50 MPa and H5 at 60 MPa, while for all kenaf it is only 16 MPa. The fraction H4 (32/68) showed the best strain value at 14%, indicating that an increase in the natural fiber fraction led to a higher strain value. Moreover, H1, H2, and H5 also demonstrated strains ranging from 11 to 12%. Based on these results, it was concluded that the combination of synthetic hybrid composites and natural fibers has good tensile and strain resistance suitable for composite products (Yahaya et al, 2014). The evolution of fiber composites, incorporating both natural and synthetic fiber reinforcement, has been extensively documented (Iqbal et al., 2020; Iqbal et al., 2022; Iqbal et al., 2023).



A previous study has explored the effect of varying the volume fraction of hollow glass micro-sphere composite lamina, hybridized with woven fiber reinforcement on tensile and bending characteristics. Several investigations have been carried out to obtain a composite material that can combine two physical forms, namely long fibers and circular/spherical particles, a hybrid composite material of glass fiber and sand particles (Rasindradita & Berata, 2013). Consequently, this study aimed to assess the tensile strength, yield strength, and elongation due to the influence of variations in sand diameter in hybrid composites reinforced by fiberglass and sand.

## 2. Materials and Methods

In this study, methyl ethyl ketone peroxide (MEKPO) was used as a catalyst to speed up the forming and curing processes. Glass fiber matt 300 and mixed sand were used as the hybrid composite reinforcement, with the typical diameters ranging from #12 (0.28 mm), #16 (0.35 mm), #20 (0.26 mm), #24 (0.24 mm), and #40 (0.22 mm) (mesh size).

The materials used also included unsaturated polyester (UP), a specific thermosetting with several applications, ranging from basic mechanical techniques, namely vacuum bags, press molding, and injection molding to more intricate processes such as hand layup. Due to its inexpensive cost, rapid drying time, clear color, good dimensional stability, and simplicity of handling, this resin is commonly used for composite applications (Berthelot, 1997). Although the use of MEKPO hardener accelerates the curing of UP resin at higher temperatures, excessive addition of catalyst can result in heat generation, leading to damage or quality loss of the composite product.

The matrix was created by combining Yukalac 157 BQTN-EX polyester with MEKPO catalyst at a ratio of 1% to the resin content. Subsequently, the solution was stirred for an additional 30 minutes at room temperature with a clean hand and was allowed to stand for 45–60 minutes for bubbles to dissipate. This process was carried out to obtain a matrix suitable for use in the creation of composite products.

According to ASTM D638 standard, tensile test pieces were cut from the composite hybrid sample panels, using Type I specifications as shown in Table 2 and Figure 1. The tensile test was carried out to determine the value of tensile strength, strain-to-failure, and elastic modulus. The results for each specimen were expressed as an average after testing through the Universal Testing Machine (UTM) three times for each variation. Subsequently, a digital microscope was used to observe the fracture profile, with all experiments and observations conducted at room temperature.

The linear equation for the relationship between stress and strain was expressed as described in Formula 1. Stress could be interpreted as the ratio between load divided by the initial cross-sectional area, as presented in Formula 2. Meanwhile, strain represented the deviation between the final length and the initial length, divided by the initial length, and multiplied by the percentage, as shown in Formula 3. The modulus of elasticity is an index used to measure the resistance of a material to elastic deformation when a load is applied, by comparing stress with strain.

**Table 1** Dimension of tensile test specimen according to ASTM D638.

Dimension	Type I (in mm) for T-Thickness of specimen ≤ 7
W-width of reduced section	13
L-Length of reduced section	57
W <sub>0</sub> -Width of the grip area	19
L <sub>0</sub> -Overall length	165
G-Length of gage	50
D-Distance between grips	115
R- Fillet radius	76

Source: Ilman et al (2018).

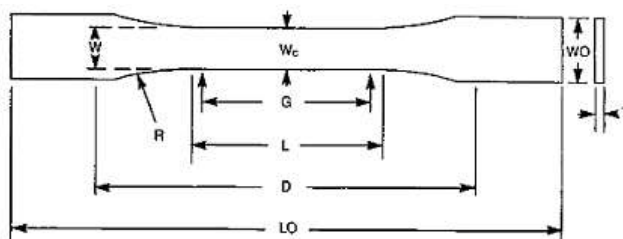


**Figure 1** Tensile test specimen of ASTM D638.

Source: Ilman et al (2018).

$$\sigma = E \times \varepsilon \tag{1}$$

$$\sigma = \frac{F}{A_0} \tag{2}$$

$$\varepsilon = \frac{\Delta L}{L_0} \times 100\% \tag{3}$$



where  $\sigma$  is the tensile strength (N/mm<sup>2</sup>), F is the load (N), A<sub>0</sub> is the initial surface area (mm<sup>2</sup>), E is the modulus of elasticity (GPa),  $\epsilon$  is the strain (%),  $\Delta L$  deviation of final -initial length (mm), and L<sub>0</sub> initial length (mm).

Figure 2 illustrates the placement of a matt 300-matt mixed sand-glass fiber matrix combined with sand-matrix used in composite production utilizing the hand lay-up method. When the fiber and sand were manually laid out, a press molding procedure was carried out for 24 hours at room temperature.

The sand was mixed with five different diameters, ranging from 12, 16, 20, 25, and 40 mm to create composite materials reinforced with glass fiber. To ensure a precise drying process of the composite material, both on the surface and inside, the final composite was removed from the mold, resulting in sheet-shaped products that were post-cured at 60°C for 30 minutes. As illustrated in Figure 2, the composite material was cut to the specifications for the ASTM D 638 tensile test, and prepared for the experiment.

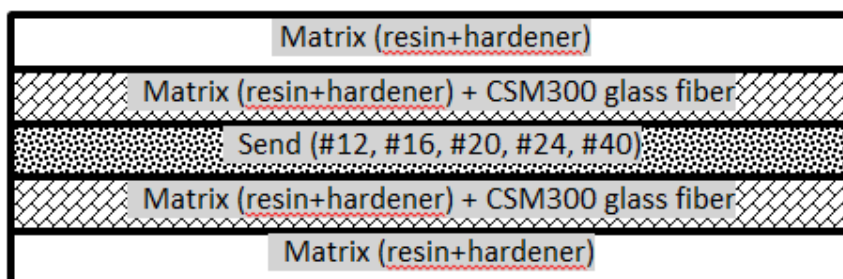


Figure 2 Schematic of the places of the fiber and matrix arrangements.

### 3. Results

Based on Figure 3a, the average yield stress index due to variations in the diameter of the sand particles, ranging from #12, #16, #20, #25, and #40, was 34.792, 44.842, 29.634, 20.614, and 17.534 MPa, respectively. The results showed that a reduction in the diameter of the sand size increased the yield stress, reaching a maximum of 44.84 MPa in #16 mesh. However, the values obtained decreased with higher grain size, or increasing mesh size (#), indicating a reduction in the tensile strength index as the diameter increases.

The results of the average maximum tensile test from the data are presented in Figure 3b. Across the mesh sizes ranging from #12 to #40, the effects of varying the diameter of the sand particles were found to be 38.508, 49,496 32,714 22.338 MPa, and 19.207 MPa, respectively. Initially, it was observed that the tensile strength increased as the sand diameter reduced, reaching a maximum of 49.49 MPa at mesh #16. However, as the sand diameter was further reduced, the tensile test value decreased. This trend indicated that a reduction in diameter correlated with a decreased tensile strength index.

As presented in Figure 3c, the percent elongation due to variations in the diameter of the sand grain particles ranging from mesh #12 to #40 was 10.175, 9.737, 9.189, 6.996, and 6,096 (%), respectively. These results showed that the percent elongation decreased with increasing sand size diameter, reaching a maximum of 10.17% in #12 mesh.

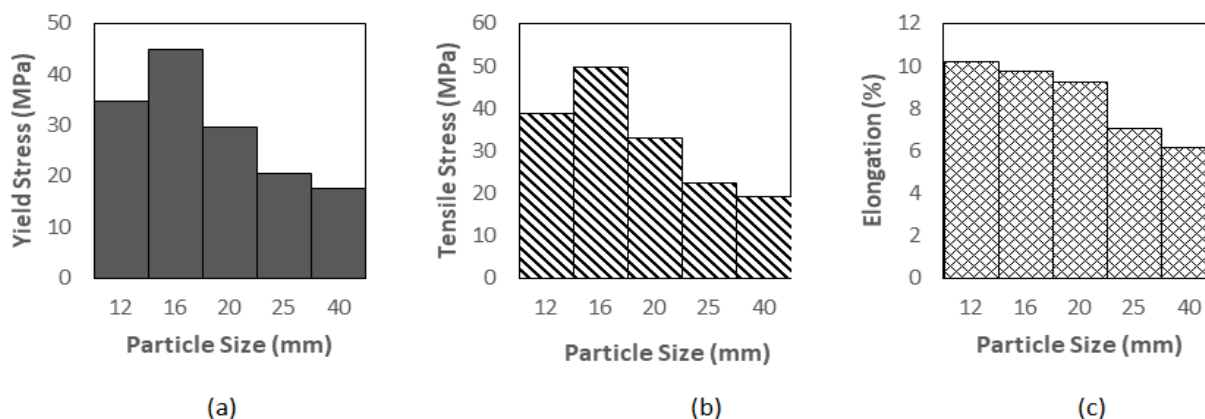
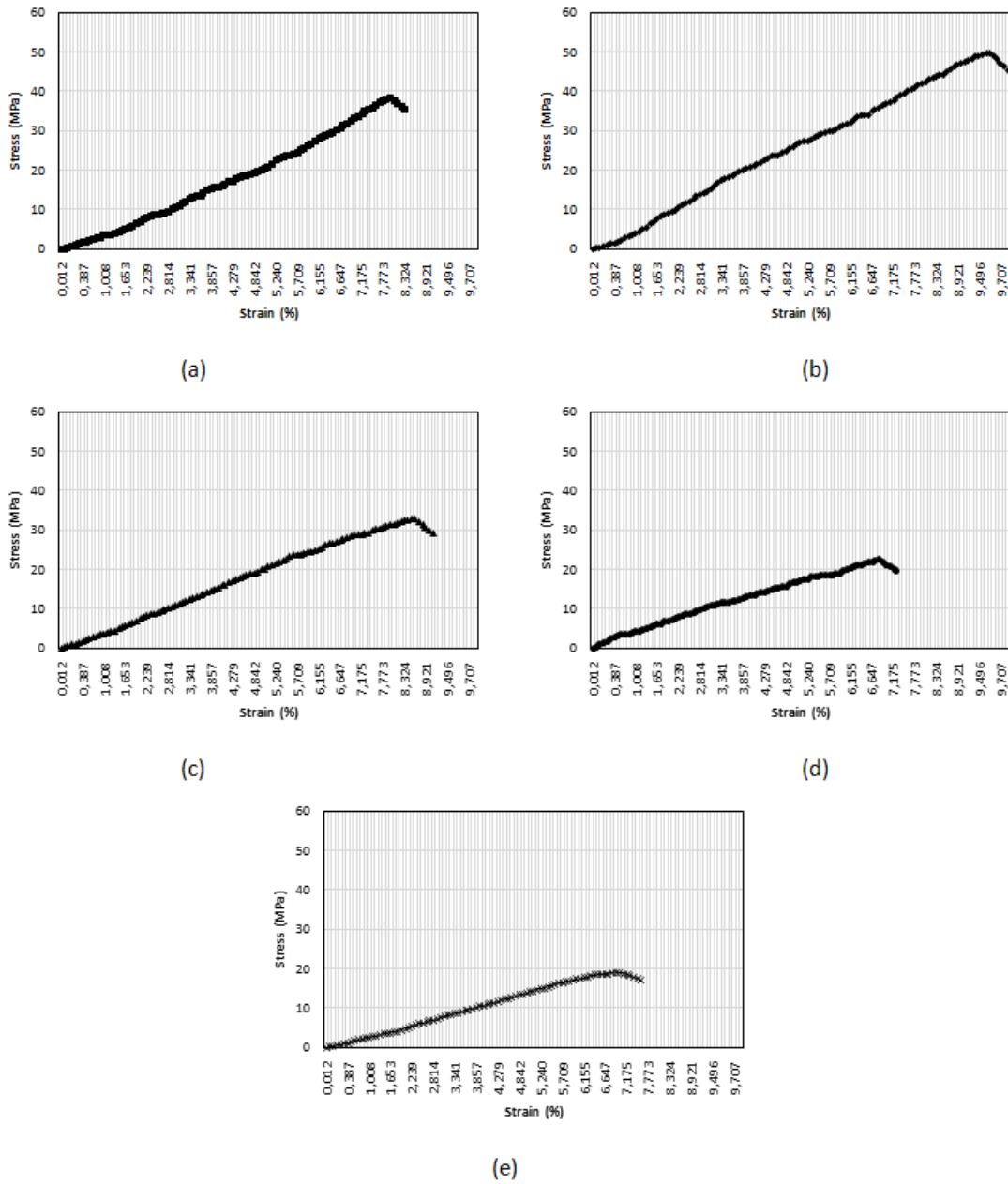


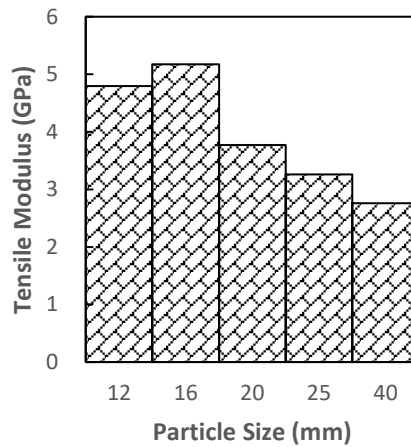
Figure 3 (a) Yield stress vs. sand particle size, (b) Tensile stress vs. sand particle size and (c) Elongation vs. sand particle size.

Figure 4 summarizes the fracture patterns after the tensile test and shows typical stress-strain curves for each sample set with different sand diameter sizes. All measurement curves show approximately linear behavior with a slight decrease, indicating the influence of composite variations in sand sizes on the strength of the grains and fibers within the matrix. These composites form covalent bonds through adhesion, establishing bonds between various types of elements on the sand (ceramic) surfaces.





**Figure 4** Stress-strain curves of tensile test samples with different sand sizes (various mesh sizes): (a) #12/0.28 mm, (b) #16/0.35 mm, (c) #20/0.26 mm, (d) #25/0.24 mm, and (e) #40/0.22 mm.



**Figure 5** Tensile modulus with different sand sizes.

The highest tensile modulus was observed in #16 mesh sand, specifically at 5.17 GPa, while the lowest elastic modulus of 2.76 GPa was found in the hybrid composite product, with the addition of #40 mesh sand. These results showed that as the elastic modulus decreased, the mesh size (sand size diameter) increased. Moreover, the tensile modulus, also known as the elasticity measure of solid material, is a mechanical characteristic expressed as the ratio of strain representing the relative deformation to tensile stress (the force per unit area) during elastic deformation of the material.

#### 4. Discussion

The tensile stress value varied depending on the grain size, with #16 sand showing a higher tensile strength compared to other diameters/meshes. This variation was attributed to the weakening of the interfacial bond between the sand and the matrix due to the smaller size, resulting in decreased tensile strength. According to the theory of rigid body equilibrium, the placement of the filler in the matrix results in an even center of gravity and a moment of inertia (mass distribution on the tensile specimen) at each position point for the fiber arrangement (Akhyar, 2018).

The operational processes of structural dynamic material damping in fabric-reinforced composites were also examined in this study. Although the mesomechanic geometry of fabrics was not adequately considered by relatively basic homogenization procedures, it significantly affected the structural dynamic material properties (Romano et al., 2017). The effect of temperature during the manufacturing process also affected the tensile strength (Akhyar et al., 2022). Coir fiber with varying fiber content was selected as reinforcements to prepare polymer-based matrices. To address the problem of reduced fiber-matrix inter-facial bond strength, the chemical treatment of coir fibers with an alkali solution was investigated. The results showed that the impact strength of coir fiber-reinforced polyester composite mainly depended on fabrication factors such as fiber-polyester content, soaking period, agent concentration, and adhesive interaction between the fiber and reinforcement (Karthikeyan, 2021). The stiffness behavior of hybrid laminated composites with surface cracks has also been evaluated and the results were shown as force-time and force-displacement graphs that fluctuate over time. Consequently, the impacts of stacking sequence on hybrid composite plates were further investigated (Günes & Sahin, 2016) and Günes and Sahin, 2016).

The dispersion of sand particles in a fiberglass-reinforced composite matrix can increase tensile strength by influencing the direction of crack propagation. However, the strength of the sand-fiberglass hybrid composites can be compromised when the bond between the surface of the sand and the matrix interface is insufficient. Since sand is a brittle and easily separated type of ceramic, this experiment shows that the contact between the sand surface and the matrix is not relatively strong. This indicates that the tensile strength of the sand-fiberglass hybrid composite decreases as the sand size increases.

This study investigated the use of sisal fiber and organic polymer polyurethane to enhance the direct tensile strength (DTS) of sand. The results showed that sand DTS significantly increased with higher fiber and polymer concentrations. The coating, bonding, and surface-filling effects of the polymer matrix significantly improve interfacial interactions, creating a cohesive environment that facilitates the use of fiber strength (Ma et al., 2022). The production of high-strength seawater sea-sand engineered cementitious composites (SS-ECC) was also investigated. The results showed that the tensile strain capacity increased with high fiber length and the tensile performance of SS-ECC was significantly independent of sea sand size (Yu et al., 2021). In recent years, several investigations have employed coarse silica sand to substitute the use of ultrafine in reducing the shrinkage of designed cement composites. The impacts of varying particle sizes of silica sand on the tensile characteristics were also examined. Based on the results, silica sand with a greater particle size showed more pores and a looser matrix, which hindered fiber dispersion and fiber/matrix interfacial bonding, thereby reducing tensile strength (Lu et al., 2023). Furthermore, the analysis investigated the impact of sand size on the mechanical properties of cement-based composites with nano-SiO<sub>2</sub> (NS) and polyvinyl alcohol (PVA) fibers. The results showed that the workability and tensile strength of PVA-reinforced composites containing NS were reduced by finer sand (Ling et al., 2020).

#### 5. Conclusions

In conclusion, this study investigated the impact of varying sand diameters on the tensile strength of composites reinforced with fiberglass and sand. The analysis showed that the hybrid system with both types of glass fiber and sand at a diameter of #16 had the maximum tensile strength (RS+FG-SP#16-FG+RS: 49.49 MPa) (sand mesh size). For the #16 and #12 sand mesh sizes, the maximum yield stress and percent elongation were 44.84 MPa and 10.17%, respectively. The greatest tensile strain-to-failure for the fiberglass hybrid composite was observed at #16 sand mesh particle size, increasing significantly from 0.22% at the beginning of the mesh particle size variation. However, the tensile strength declined as the sand diameter became more refined, peaking at 0.35 mm (#16). This reduction in the strength of sand-fiberglass hybrid composites occurred due to insufficient contact between the sand surface and matrix interface. This study demonstrates that the interaction between the sand surface and the matrix is not relatively strong because the sand behaves as a ceramic material that is fragile and readily separated. Consequently, as sand size increases, the tensile strength of the sand-fiberglass hybrid composite decreases. The results showed a regular trend suggesting that the elastic modulus decreased with an

increasing mesh size (sand particle diameter), indicating a reduction in the yield stress, tensile stress, and elastic modulus as the sand particle diameter increased.

### Ethical considerations

Not applicable.

### Conflict of Interest

The authors declare no conflicts of interest.

### Funding

This publication was made possible by a grant from the Research Fund of the Ministry of Research, Technology, and Education, Republic of Indonesia, and the Institute for Research and Community Services (LPPM) Universitas Syiah Kuala; the financial support is greatly appreciated. We would like to thank Mr. Rizwan for their support during this experiment.

### References

- Akhyar, Iswanto, P. T., Malau, V. (2022). Impact of pouring temperature on the mechanical properties of Al5.9Cu1.9Mg alloy. *Archives of Materials Science and Engineering*, 113(2):49-55, DOI: 10.5604/01.3001.0015.7016.
- Akhyar, H., Iswanto, P. T., Malau, V. (2018). Non Treatment, T4 and T6 on Tensile Strength of Al-5.9Cu-1.9Mg Alloy Investigated by Variation of Casting Temperature. *Materials Science Forum*, 929:56–62, <https://doi.org/10.4028/www.scientific.net/msf.929.56>.
- Alavudeen, A., Rajini, N., Karthikeyan, S., Thiruchitrambalam, M., Venkateshwaren, N. (2015). Mechanical properties of banana/kenaf fiberreinforced hybrid polyester composites: Effect of woven fabric and random orientation. *Materials & Design*, 66:246-257.
- Berthelot, J. M. C. (1999). Composite Materials Mechanical Behavior and Structural Analysis, Semantic Scholar, Corpus ID:135854013.
- Güneş, A., Şahin, Ö. A. (2016). Stiffness behavior of hybrid laminated composites with surface crack. *Archives of Materials Science and Engineering*, 80(2):49-52, DOI: 10.5604/18972764.1229632
- Güneş, A., Şahin, Ö. A., (2016). Effect of surface crack depth on hybrid laminated composites. *Archives of Materials Science and Engineering*, 82(1):38-41, DOI: 10.5604/18972764.1229698
- Ilman, K. A., Jamasri, K., Hestiawan, H. (2018). The Tensile Strength Evaluation of Untreated Agel Leaf/Jute/Glass Fiber-Reinforced Hybrid Composite, The 2nd Annual Applied Science and Engineering Conference (AASEC 2017), *IOP conference series: materials science and engineering*, 288:012088, doi:10.1088/1757-899X/288/1/012088
- Iqbal, M., Aminanda, Y., Firsya, T., Ali. M. (2020). Bending strength of polyester composites reinforced with stitched random orientation and plain weave abaca fiber. *IOP conference series: materials science and engineering*, 739(1):012035.
- Iqbal, M., Aminanda, Y., Firsya, T., Nazaruddin, N. I. S., Erawan, D. F., Saputra, D. A., Nasution, A. R. (2023). The effect of fiber content and fiber orientation on bending strength of abaca fiber reinforce polymer composite fabricated by press method. *AIP Conference Proceedings*, 2643(1): 050055.
- Iqbal, M., Azan, S. A., Rahmadtullah, R., Abhang, L. B. (2022). Flexural Strength and Physical Properties of Cement Board Reinforced with Abaca Fiber. *Key Engineering Materials*, 930: 169-178.
- Karthikeyan, S. (2021). Influence of fibre loading and surface treatment on the impact strength of coir polyester composites. *Archives of Materials Science and Engineering*, 107(1):16-20, DOI: 10.5604/01.3001.0014.8190
- Rasindradita, M., Berata, W. (2013). Pengaruh Penambahan Prosentase Fraksi Volume Hollow Glass Microsphere Komposit Hibrida Lamina dengan Penguat Serat Anyaman Terhadap Karakteristik Tarik dan Bending. Tugas Akhir Teknik Mesin, FTI- ITS, Surabaya (In Indonesia).
- Romano, M., Ehrlich, I., Gebbeken, N. (2017). Structural mechanic material damping in fabric reinforced composites: a review. *Archives of Materials Science and Engineering*, 88(1):12-41, DOI: 10.5604/01.3001.0010.7747
- Yahaya, R., Sapuan, S. M., Jawaid, M., Leman, Z., Zainudin, E. S. (2014). Mechanical performance of woven kenaf-Kevlar hybrid composites. *Journal of Reinforced Plastics and composites*, 33(24):2242-2254.